

# 1 **Frequency of large volcanic eruptions over the past 200,000 years**

2

3 Eric W. Wolff<sup>1</sup>, Andrea Burke<sup>2</sup>, Laura Crick<sup>2</sup>, Emily A. Doyle<sup>1</sup>, Helen M. Innes<sup>2</sup>, Sue H. Mahony<sup>3</sup>, James  
4 W.B. Rae<sup>2</sup>, Mirko Severi<sup>4</sup> and R. Stephen J. Sparks<sup>3</sup>

5 <sup>1</sup>Department of Earth Sciences, University of Cambridge, Cambridge CB2 3EQ, United Kingdom

6 <sup>2</sup>School of Earth & Environmental Sciences, University of St Andrews, St Andrews, KY16 9AL, United Kingdom

7 <sup>3</sup>School of Earth Sciences, University of Bristol, Bristol BS8 1RJ, United Kingdom

8 <sup>4</sup>Chemistry Department, University of Florence, Sesto F.no (FI) 50019, Italy

9 *Correspondence to:* Eric W. Wolff (ew428@cam.ac.uk)

10 **Abstract.** Volcanic eruptions are the dominant cause of natural variability in climate forcing on timescales up to multidecadal.  
11 Large volcanic eruptions lead to global-scale climate effects and influence the carbon cycle on long timescales. However,  
12 estimating the frequency of eruptions is challenging. Here we assess the frequency at which eruptions with particular deposition  
13 fluxes are observed in the EPICA Dome C ice core over the last 200 kyr. Using S isotope analysis we confirm that most of the  
14 largest peaks recorded at Dome C are from stratospheric eruptions. The cumulative frequency through 200 kyr is close to linear  
15 suggesting an approximately constant rate of eruptions. There is no evidence for an increase in the rate of events recorded in  
16 Antarctica at either of the last two deglaciations. Millennial variability is at the level expected from recording small numbers  
17 of eruptions, while multimillennial variability may be partly due to changes in transport efficiency through the Brewer-Dobson  
18 circulation. Our record of events with sulfate deposition rates  $> 20 \text{ mg m}^{-2}$  and  $>50 \text{ mg m}^{-2}$  contains 678 and 75 eruptions  
19 respectively over the last 200 kyr. Calibration with data on historic eruptions and analysis of a global Quaternary dataset of  
20 terrestrial eruptions indicates that sulfate peaks with deposition rates  $> 20 \text{ mg m}^{-2}$  and  $>50 \text{ mg m}^{-2}$  correspond to explosive  
21 eruptions of magnitude  $\geq 6.5$  and  $\geq 7$  respectively. The largest recorded eruption deposited just over  $300 \text{ mg m}^{-2}$ .

## 22 **1. Introduction**

23 Volcanic eruptions can have devastating local effects, and at a global scale they are one of the important natural components  
24 of forcing in the climate system (Robock, 2000). The forcing arises from sulfate aerosol that is formed from  $\text{SO}_2$  erupted into  
25 the stratosphere. On longer timescales the balance between volcanism and weathering controls the  $\text{CO}_2$  content of the  
26 atmosphere, and changes in volcanic eruption frequency could contribute to the changes in  $\text{CO}_2$  concentration observed at  
27 glacial terminations (Huybers and Langmuir, 2009). In order to constrain changes in forcing by volcanic aerosol, as well as  
28 any role of volcanoes in glacial-interglacial  $\text{CO}_2$  change, a key question is whether global eruption rate is steady and, if not,  
29 whether any variation is related to climate.

30 There has been much interest in the notion that rates of explosive volcanism have been moderated by processes related to  
31 climate change (Kutterolf et al., 2019; Watt et al., 2013). Rates of mantle melting are expected to be affected by glacial cycles:

32 melting of ice caps leads to unloading, enhanced mantle melting and enhanced volcanism (Huybers and Langmuir, 2009; Jull  
33 and McKenzie, 1996). Rates of volcanism might also be affected by sea level change (Huybers and Langmuir, 2009; Kutterolf  
34 et al., 2019). Over very long timescales, changes in plate tectonics and occurrence of mantle plume volcanism are expected to  
35 be reflected in rates of volcanism.

36 Beyond the period of direct historic observations, explosive eruptions are recorded as tephra deposits in terrestrial and marine  
37 records, and as both sulfate and occasional tephra deposits in ice cores. Terrestrial tephra deposits give information about  
38 location as well as strength and frequency of eruptions (Brown et al., 2014), but they are notoriously difficult to use, and a  
39 statistical approach is needed to turn them into useful measures of eruption frequency (Rougier et al., 2018). Tephra in marine  
40 cores offers a further opportunity to compile eruption statistics (Mahony et al., 2020), but it is also challenging to compile a  
41 record that is unbiased over time and space. Eruptions are also recorded as sulfate deposition in ice cores. While this provides  
42 no direct information on the location and magnitude of each eruption, it can be used to log eruptions relevant for climate  
43 forcing (Gao et al., 2008; Sigl et al., 2015). There have been only limited investigations (Castellano et al., 2005; Castellano et  
44 al., 2004; Cole-Dai et al., 2021; Lin et al., 2022) to estimate volcanic eruption occurrence from ice core data beyond the last  
45 2500 years.

46 Although records from both poles may be combined to identify explosive eruptions recorded at both poles (and therefore most  
47 likely having reached the stratosphere), the use of Greenland ice core records alone is complicated, because they are dominated  
48 by the relatively local input from Icelandic eruptions. For the region around Antarctica, there are active volcanoes in New  
49 Zealand, the Andes, the South Sandwich and South Shetland Islands, and within the continent in Marie Byrd Land and around  
50 McMurdo Sound. However the frequency of large eruptions from these areas is expected to be low (notwithstanding an unusual  
51 event at the last deglaciation (McConnell et al., 2017)), and the local sources within the continent are far from Dome C. The  
52 record of eruptions is therefore likely dominated by those that have reached the stratosphere and have a global climate effect.

53 Eruptions can be logged using spikes in sulfate, or as a surrogate, spikes in the dielectric profile conductance (DEP) or low  
54 frequency electrical conductivity (ECM) of ice (Wolff, 2000), both of which respond to acidity in the ice. Such records are  
55 available continuously from a number of ice cores on the East Antarctic plateau. Issues of resolution and diffusion mean that  
56 the volcanic spikes cannot be reliably observed to the bottom of the cores, but they are clearly identified over at least the last  
57 two glacial cycles. This has for example allowed their use to synchronise age models to 128 ka bp between EPICA cores at  
58 Dome C (EDC) and Dronning Maud Land (EDML) (Ruth et al., 2007), to 145 ka between EDC and Vostok (Parrenin et al.,  
59 2012), and to 216 ka between EDC and Dome F (Fujita et al., 2015).

60 Several issues make it challenging to construct a consistent record of sulfate deposition throughout an ice core. Firstly, there  
61 is a background of sulfate from non-volcanic sources (mainly sea salt and marine biogenic). Because this background, and its  
62 variability, changes with climate, methods which merely seek outliers (Castellano et al., 2004) risk recording volcanic events  
63 depositing a particular amount of sulfate in some climate periods and not in others. Secondly there is a very large amount of

64 variability in the amount of sulfate deposited in the small footprint of snow surface sampled by an ice core (Gautier et al.,  
65 2016; Wolff et al., 2005), so that the sulfate signal of individual eruptions in a single core is subject to great uncertainty.  
66 Thirdly, despite the lower frequency of local eruptions, Antarctic ice cores will still record some of these minor eruptions  
67 which did not reach the stratosphere but are smaller eruptions of more regional origin. These can in principle be filtered using  
68 sulfur isotope analysis to identify mass independent fractionation (Baroni et al., 2008; Burke et al., 2019; Gautier et al., 2019;  
69 McConnell et al., 2017; Savarino et al., 2003a).

70 A final issue is related to resolution and diffusion. Snow accumulation rates at the East Antarctic sites mentioned above (Dome  
71 Fuji, EDC, Vostok and EDML) vary from 2-6 cm water equivalent at the different sites in the present day and are typically  
72 less than 50% of that in the last glacial maximum. Eruption signals are generally recorded above background for only 2-3  
73 years. It is therefore essential to use only data with a good depth resolution (at EDC resolution of better than 5 cm is optimal),  
74 and to estimate the flux across the peak and not just at the maximum, which will certainly be modulated by the resolution.  
75 Additionally sulfate peaks diffuse with age (Barnes et al., 2003), and we find that volcanic peaks that were just a few years  
76 wide on deposition may appear to be 20 years wide in ice of 200 ka age at EDC. This is helpful because it means that, as layers  
77 thin with depth, the decreasing age resolution of our measurements is not a limiting factor. However it makes it yet more  
78 challenging to identify eruptions of a particular scale in a consistent way, because peaks that stand clearly above background  
79 in recent ice diffuse towards the background in older ice.

80 It is also important to be aware that even a perfect record of sulfate deposition events is not easy to convert into a record of  
81 eruption magnitude and frequency. In addition to the strength of the eruption, sulfate deposition depends on the sulfur content  
82 of the eruption, the latitude of the volcano and atmospheric transport processes (Marshall et al., 2021). Finally, there are  
83 difficulties in converting sulfate loading in an ice core to the magnitude (defined by volcanologists as magma mass erupted).  
84 Eruption magnitude is only one of several factors that influence sulfate mass released in explosive eruptions (Wallace and  
85 Edmonds, 2011).

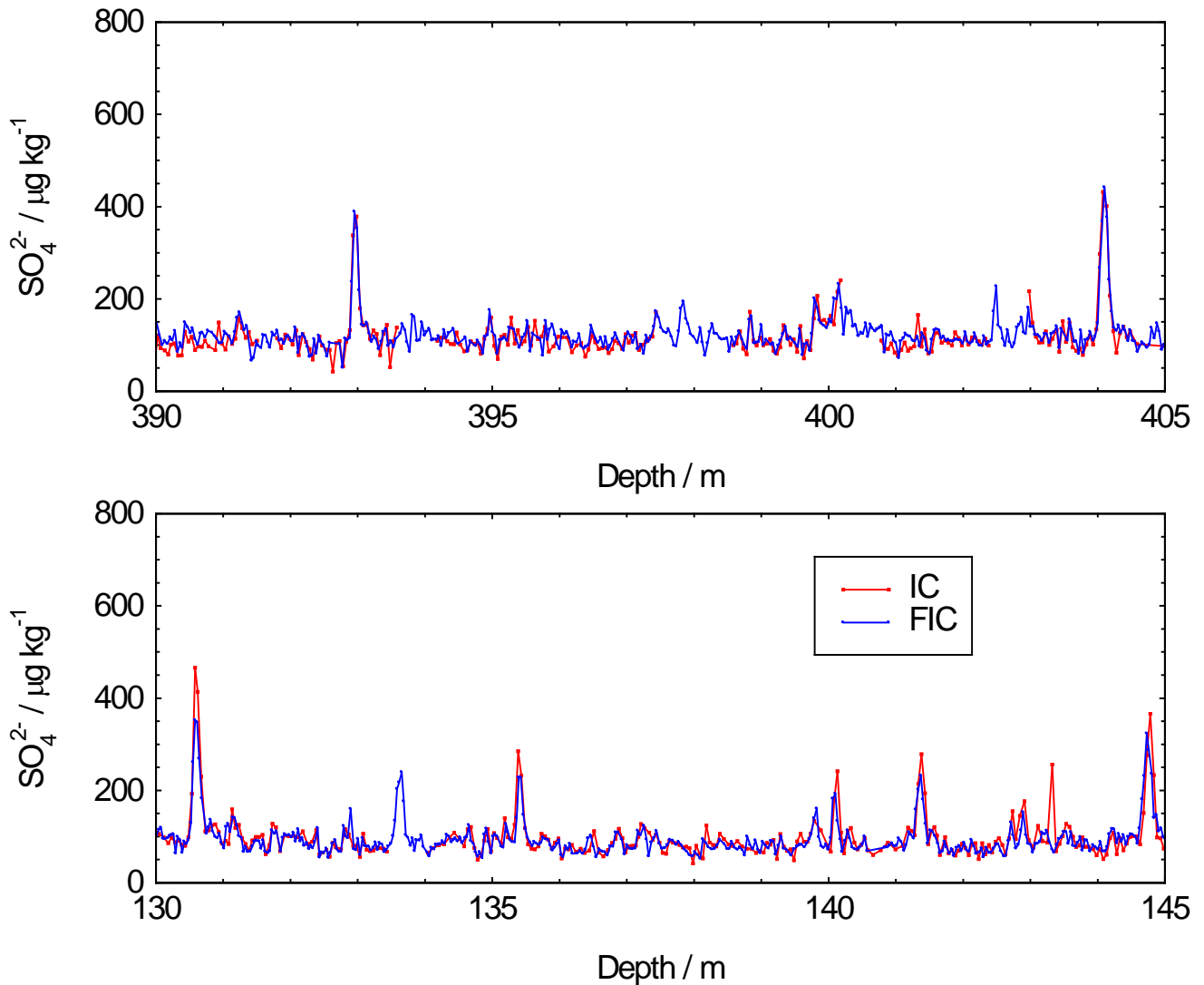
86 Despite these problems two recent papers (Cole-Dai et al., 2021; Lin et al., 2022) have attempted to assess eruption frequency.  
87 One (Cole-Dai et al., 2021) examined the number of eruptions recorded in the WAIS Divide core over the last 11 kyr, observing  
88 variability but no trend in eruption rate. A second (Lin et al., 2022) assessed eruption frequencies recorded in both Greenland  
89 and Antarctica over the period from 9-60 kyr ago, and compared them with the rates in the last 2 kyr. For Greenland they  
90 found relatively constant rates of eruption through time, but with a small increase in frequency of recorded eruptions across  
91 the deglaciation (21-9 ka). This is consistent with the idea that the removal of ice from high latitude eruption regions, with a  
92 particular emphasis on Iceland (Jull and McKenzie, 1996), would have led to an increased eruption rate recorded in Greenland.  
93 For Antarctica, using methods similar to those we describe later, the authors (Lin et al., 2022) found no significant change in  
94 eruption rate across the 60 kyr period.

95 In this paper we log eruption frequencies from the Antarctic ice core of EDC to 200 ka, using a methodology that assesses the  
96 scale of sulfate deposition consistently with depth, age and climate period. We use this to assess the variability in recorded  
97 eruptions with time and with climate. We discuss how representative the eruption record in Antarctica is, and use sulfur isotope  
98 analysis to augment this discussion.

## 99 **2. Data**

100 Sulfate was measured along the EPICA Dome C (EDC) ice core by two methods, standard ion chromatography (IC) and fast  
101 ion chromatography (FIC) (Littot et al., 2002; Severi et al., 2015). FIC measurements were at higher resolution (typically 5-6  
102 cm in the top 100 m, 3-5 cm below that to 770 m, and 2 cm below 770 m) than IC measurements; additionally there are sections  
103 of the core where IC data are not available. For these reasons FIC data were preferred.

104 However, although initial tests had suggested good agreement between the methods (Littot et al., 2002), a more detailed  
105 analysis suggested some calibration problems during the first field season of FIC use, to a depth of 358.6 metres (11745 years  
106 before present (1950) on the AICC2012 age model). In this depth range we consider the well-established IC method to be more  
107 reliable. Detailed comparison of FIC and IC data was carried out where both were available. While it is impossible to diagnose  
108 exactly what the issue was, a plot of FIC data against IC data for values more than  $50 \mu\text{g kg}^{-1}$  above the background showed a  
109 gradient of 0.70 for data between 0 and 358.6 m, and 0.94 between 360 m and 720 m. This is shown in Fig. 1 and was used as  
110 justification to multiply the FIC values above background (i.e. the residual after subtracting the background) by (1/0.7) for  
111 data above 358.6 m (<11.7 ka) during the data processing.

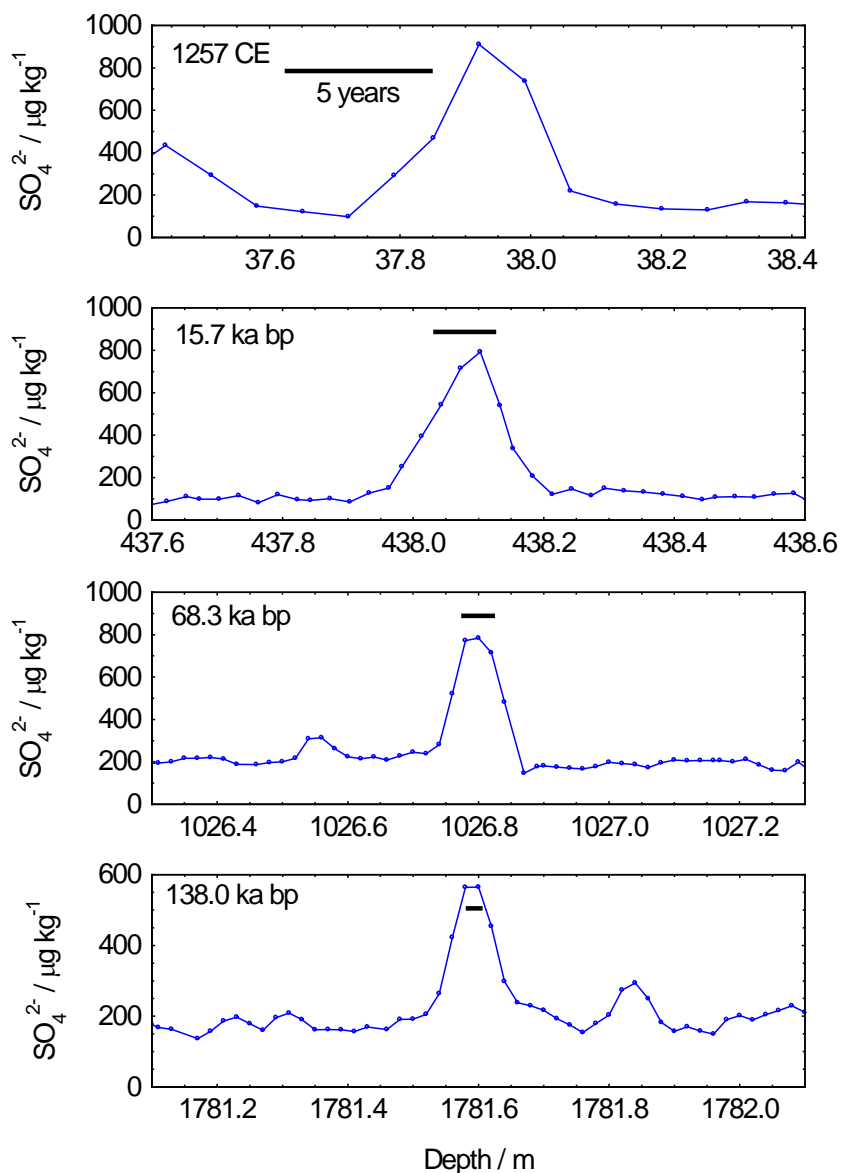


112

113

114 **Figure 1.** Comparison of FIC and IC data for two sections of the EDC ice core. In the section from 130 to 145 m, FIC peaks are consistently  
 115 lower than those of IC while in the section from 390 metres, the concentrations are essentially the same in the two methods.

116 Beyond 358.6 m, the data were used without correction. Volcanic peaks, standing clear of the sulfate background, remain  
 117 visible beyond 200 ka. It is clear that diffusion has occurred, making peaks considerably wider in years (and consequently  
 118 smaller in amplitude) than they were at the time of deposition; however, thinning seems to balance diffusion rather closely  
 119 (Fig. 2). The result is that peaks remain within about a 30 cm window at all depths to 200 ka, and the resolution of the data  
 120 remains adequate to estimate peak areas.

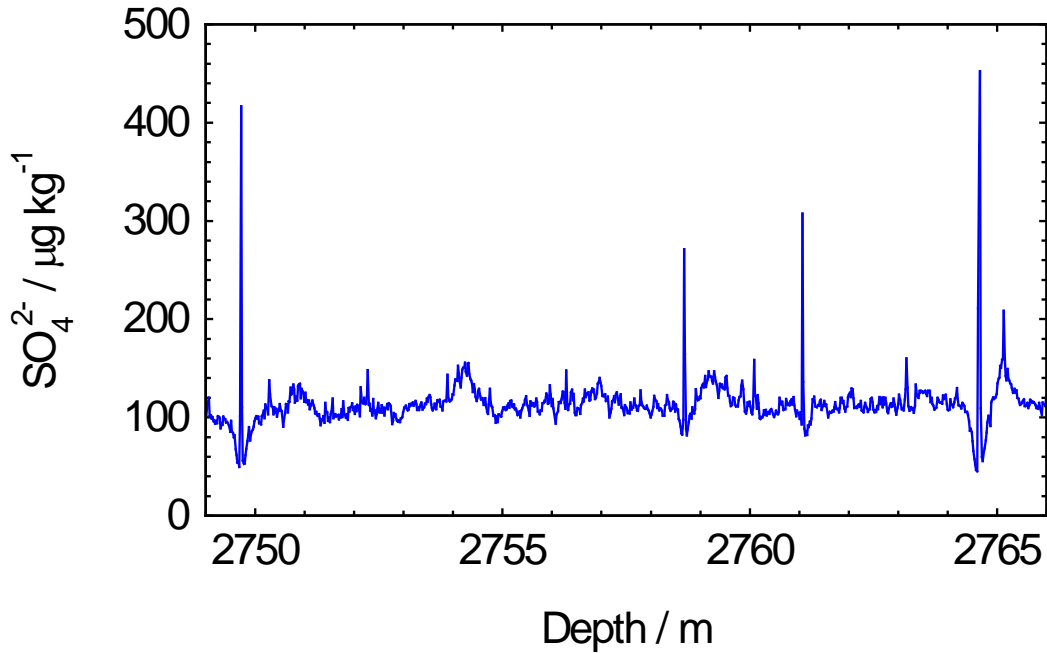


121

122 Figure 2. Examples of volcanic peaks at different depths and ages. The 1257 peak (top panel) is shown after application of the  
 123 correction described above. The black horizontal bar on each plot represents 5 years at each depth. Dots represent the mid-  
 124 depths of individual samples.

125 The dataset includes sections of missing data, where no FIC sulfate data are available. Mainly this consists of short sections at  
 126 the end of core lengths, but there are some longer sections where data were not taken either because of poor core quality or  
 127 instrument problems. Out of 2070 m of ice, there are 25 gaps longer than 30 cm, consisting in total of 19 m of ice. We discuss  
 128 our treatment of missing data under methods.

129 In deeper ice, it has been observed (Traversi et al., 2009) that anomalous spikes in sulfate concentration form through an as-  
130 yet uncharacterised post-depositional process. In Fig. 3 we show clear examples of this artefact at about 400 ka; sulfate appears  
131 to have been “sucked” from the surrounding background into a sharp peak. We observed signs of this behaviour as shallow as  
132 2500 m (300 ka). To avoid any possibility of including such artefact peaks, we restrict our subsequent analysis to the past 200  
133 kyr. This also avoids the problem that peaks become harder to distinguish from background with greater depth.



134

135 Figure 3. An example of four artefact peaks in ice aged just over 400 ka.

136 Material for the last few decades was not available in the EDC ice core because the top few metres were not retrieved. However,  
137 the Pinatubo period has been studied previously at Dome C using snow pits (Castellano et al., 2005). The observed peak  
138 (deposition of  $10.7 \text{ mg m}^{-2}$ ) encompassed both Pinatubo and the eruption of Mount Hudson in Chile, which could not be  
139 separated. However, the two eruptions have been resolved at South Pole (Cole-Dai and Mosley-Thompson, 1999), allowing  
140 a fraction of deposition in the combined peak to be assigned to each eruption. Using the same fraction, we estimate  $7.5 \text{ mg m}^{-2}$   
141 for the Pinatubo sulfate deposition at Dome C, used later as part of benchmarking our data.

### 142 3. Methods

143 We applied the following method of calculating sulfate deposition. The ice core volcanic record consists of numerous sharp  
144 spikes of sulfuric acid input, superimposed on a noisy background. The background consists mainly of sulfate from oxidation

145 of marine biogenic emissions of dimethylsulfide, with small contributions from sea salt as well as background volcanic sulfate.  
146 Based on sulfate concentration measurements (Legrand and Delmas, 1984) and measurements of  $\delta^{34}\text{S}$  in ice at South Pole  
147 (Patris et al., 2000), the volcanic contribution to the background is estimated as less than 10%. In order to calculate the sulfate  
148 deposition during each individual eruption event, we subtract the background and then sum the area across the peak, correcting  
149 for ice thinning.

150 To correct for the background, we subtracted a running median from the dataset. The median is preferred to the mean because  
151 the mean includes the volcanic peaks while the median should, if well-chosen, exclude the peaks. The time period over which  
152 the median is calculated needs to be short enough that it follows the varying background but long enough that it will never use  
153 the values within volcanic peaks. In our standard calculations we used 200 years, but other periods were also tested in  
154 sensitivity studies. Varying the period over which the median was calculated between 100 and 400 years changed the total  
155 number of peaks above a threshold of  $20 \text{ mg m}^{-2}$  by up to 10% compared to the standard case (200 years) but did not affect the  
156 profile of peaks with time.

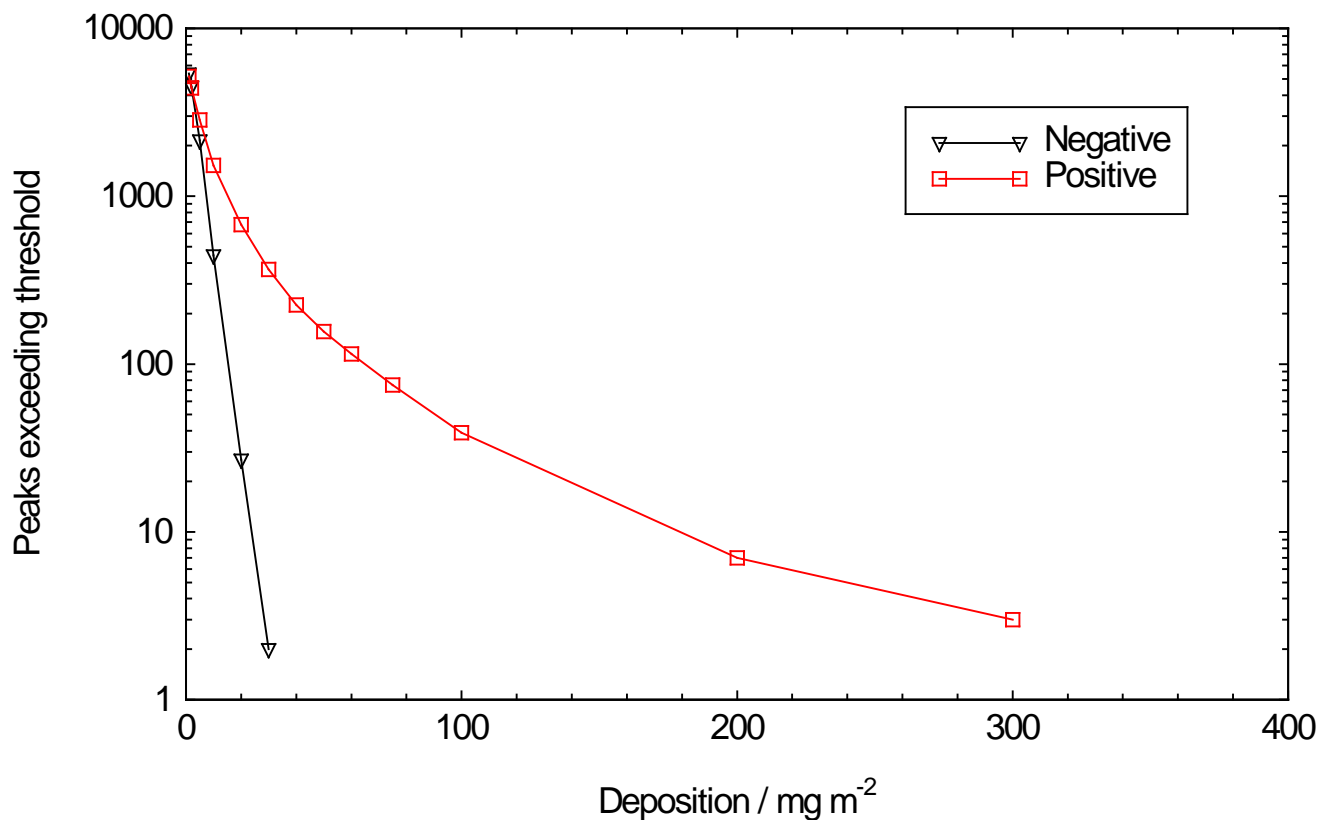
157 Having subtracted the background, we calculate the total amount of sulfate deposited to the snow per unit area across the whole  
158 eruption. A key assumption is that the sulfate is mainly deposited by dry deposition, which is expected to be true at a site like  
159 Dome C with its very low snow accumulation rate. This justifies the underlying assumption that the sulfate flux scales with  
160 the amount of sulfate injected into the stratosphere. We first calculate the annual flux of sulfate in each sample ( $\mu\text{g m}^{-2} \text{ a}^{-1}$ ) as  
161  $F = C * A$ , where  $C$  is the concentration in a slice of ice ( $\mu\text{g kg}^{-1}$ ), and  $A$  is the snow accumulation rate ( $\text{kg m}^{-2} \text{ a}^{-1}$ ). We then  
162 calculate the total deposition in each sample ( $\mu\text{g m}^{-2}$ ) by multiplying the flux by the time period represented in each sample;  
163 this is done by using the accumulation rate and thinning parameter derived in the AICC2012 age model (Bazin et al., 2013) to  
164 calculate the annual layer thickness. Finally, since the FIC data are effectively averages for discrete slices, we sum the  
165 deposition (above background) in each of the samples that contribute to a particular peak to get the total deposition for an  
166 individual eruption. This method automatically corrects the flux for the ice thinning (which is already 73% at the depth (2090  
167 m) of 200 ka ice.

168 The algorithm we use searches for local maxima in the residual (after subtraction of the background) and calculates the sum  
169 of samples across a chosen summing width across each maximum. The summing width needs to be large enough to include  
170 all the volcanic sulfate after diffusion (Barnes et al., 2003). Visual observation suggests that a width of 30 cm (ie samples  
171 within 15 cm of the concentration maximum) is appropriate at all depths between the surface and 2100 m (see Fig. 2). This  
172 suggests that diffusion approximately keeps pace with thinning at EDC. However, this width was also varied in sensitivity  
173 studies. Varying the integration width between 20 and 40 cm altered the total number of peaks above a threshold of  $20 \text{ mg m}^{-2}$   
174 by up to 10% compared to the standard case (30 cm) but did not affect the profile of peaks with time. At many depths, an  
175 integration width of 20 cm is clearly too narrow to capture the full peak, while 40 cm includes sections of background, so the  
176 uncertainty induced by this parameter is below 10%.



177 Our method calculates numerous small peaks that are caused simply by variations around the background. To estimate this  
178 variation we also calculate “negative” peaks around our median line. We then separately sum the number of peaks and negative  
179 peaks in bins exceeding particular deposition fluxes (Figure 4). At a deposition of  $10 \mu\text{g m}^{-2}$ , there is still a substantial number  
180 of negative peaks (441 in 200 kyr, compared to 1518 positive peaks). At  $20 \text{ mg m}^{-2}$ , there are very few negative peaks (28 in  
181 200 kyr compared to 678 positive peaks), suggesting that 96% of peaks we count at this level are volcanic eruption peaks, and  
182 supporting our choice of  $20 \text{ mg m}^{-2}$  as the background threshold for counting peaks. There are no negative peaks at  $40 \text{ mg m}^{-2}$ .  
183 This indicates that, while we could investigate volcanoes with lower deposition fluxes in some time periods, we should  
184 restrict ourselves to peaks above  $20 \text{ mg m}^{-2}$  in order to count peaks of similar size consistently over 200 kyr.

185 In our standard calculation we treated missing data as having the concentration of the background, i.e. those sections did not  
186 contribute to the size of volcanic peaks in which they were embedded. We also did a calculation where we set the value of all  
187 missing sections less than 30 cm thick to be the average of the adjacent samples: this increased the total count of peaks  $> 20$   
188  $\text{mg m}^{-2}$  by only 11 (out of 678). It is likely that the longer sections of missing data (25 sections  $> 30$  cm, totalling 19 m of ice)  
189 would have contained some peaks but assuming they contain the same proportion of volcanoes as the measured parts we have  
190 probably missed less than 10 peaks with deposition  $> 20 \text{ mg m}^{-2}$ .



191

192 Figure 4. Distribution of positive and negative peaks exceeding different deposition fluxes, summed over the past 200 kyr.  
 193 Sulfur isotopes were measured on discrete samples of ice cut at high resolution (every 2-3 cm) across 21 volcanic sulfate  
 194 events from Dome C between 10.1 and 96.1 ka. These included examples of both larger and smaller volcanic peaks in the EDC  
 195 core. Samples were melted and measured for concentration by ion chromatography. Based on the concentration, a volume  
 196 corresponding to 20 nmol of sulfate was dried down and purified through anion exchange columns following the method  
 197 previously described (Burke et al., 2019). Each sample was measured at least twice for  $\delta^{34}\text{S}$  and  $\delta^{33}\text{S}$  by multi-collector  
 198 inductively coupled plasma mass spectrometry, where

$$199 \delta^x\text{S} = \left( \frac{{}^x\text{S}/{}^{32}\text{S}}{\text{sample}} / \frac{{}^x\text{S}/{}^{32}\text{S}}{\text{reference}} \right) - 1$$

200 and x is either 33 or 34. Mass independent fractionation was calculated as

$$201 \Delta^{33}\text{S} = \delta^{33}\text{S} - ((\delta^{34}\text{S} + 1) * 0.515 - 1)$$

202 The uncertainty for these  $\Delta^{33}\text{S}$  measurements is 0.14‰ (2 s.d.). Only sulfate that has been in the stratosphere shows a non-  
 203 zero signal of  $\Delta^{33}\text{S}$ , and so if the maximum magnitude  $\Delta^{33}\text{S}$  across a peak is greater than 0.14‰, the eruption is considered  
 204 stratospheric.

#### 205 4. The frequency of eruptions recorded in the EDC core, Antarctica

206 A few of the most recent sulfate layers can be correlated to specific eruptions allowing some calibration of the record to the  
 207 magnitude of explosive eruptions (Gao et al., 2008; Sigl et al., 2015), but most layers cannot be linked to a source. As a  
 208 benchmark Table 1 lists four sulfate peaks in Dome C where the eruption location and magnitude are also known, including  
 209 the 1991 Pinatubo eruptions (Castellano et al., 2005). The benchmark data (all from tropical eruptions) imply that peaks above  
 210 our chosen threshold of 20 mg m<sup>-2</sup> are likely to be M>6.5 eruptions.

<b>Eruption</b>	<b>Dome C deposition (mg m<sup>-2</sup>)</b>	<b>Magnitude</b>	<b>Emission (Tg SO<sub>2</sub>)</b>
Pinatubo 1991	7.5	6.1	18
Krakatoa 1883	13.2	6.4	19
Rinjani/Samalas 1257	74.5	7.0	119
Tambora 1815	53	7.0	56

211

212 Table 1. Identified sulfate peaks in Dome C with magnitude and estimated emission (Toohey and Sigl, 2017).

213 Various attempts have been made to derive SO<sub>2</sub> emissions (in Mt or Tg of S or SO<sub>2</sub>) from ice core deposition (in mg m<sup>-2</sup> of  
 214 sulfate) (Sigl et al., 2022). However this is difficult when there is only one ice core location, and the location of the eruption  
 215 is unknown. Model studies show that the ratio of deposition in Antarctica to emissions depends on latitude of eruption, the  
 216 height the plume reaches, and the time of year of the eruption (Marshall et al., 2021). As a rough estimate using emissions  
 217 values calculated in the literature (Toohey and Sigl, 2017) we can deduce that for tropical eruptions, SO<sub>2</sub> emissions in Tg SO<sub>2</sub>

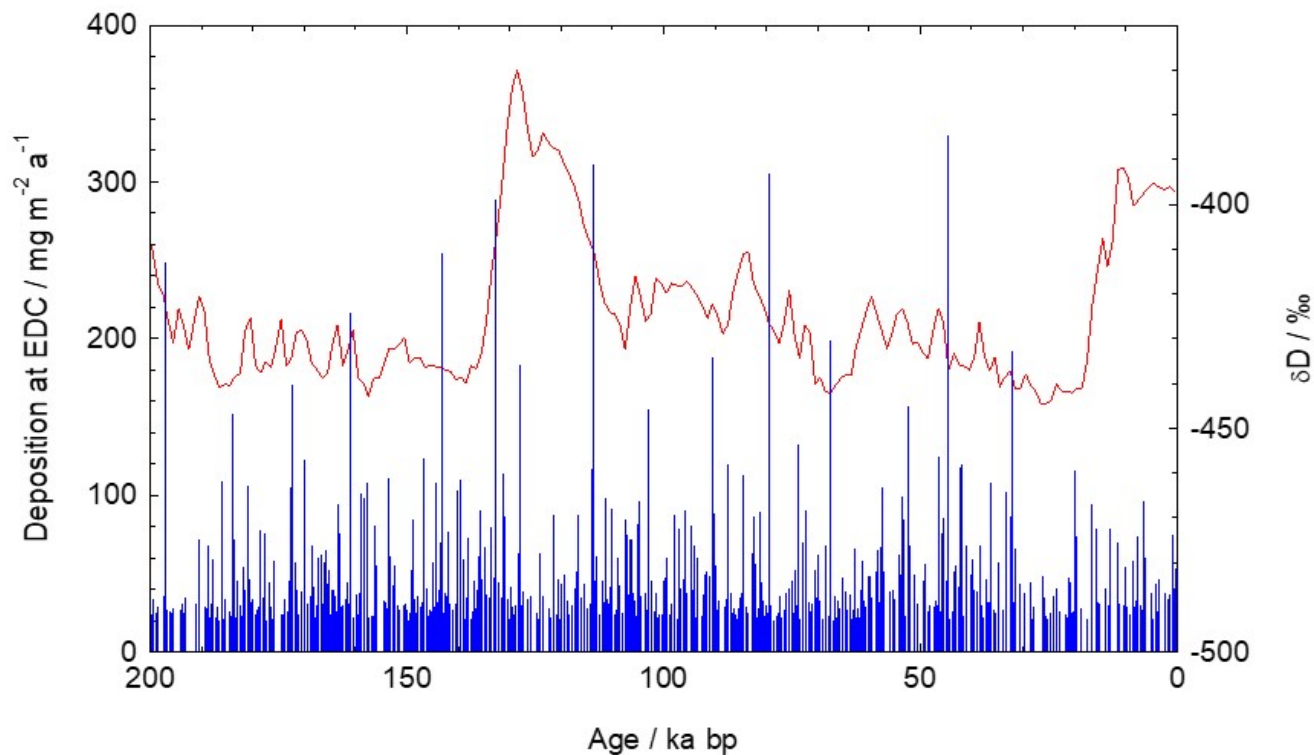
218 are about 1-2 times higher than our measured EDC depositions in  $\text{mg m}^{-2}$  (Table 1). However the factor should certainly be  
219 increased if eruptions occurred at high northern latitudes (Marshall et al., 2021).

220 It was already noted (Sigl et al., 2013; Sigl et al., 2015) that most Icelandic eruptions (such as Laki in 1783 CE and Eldgja in  
221 939 CE) that give large depositions in Greenland cannot be identified in Antarctic cores. However these eruptions are anyway  
222 estimated to be below the magnitude we would associate with depositions above our chosen threshold of  $20 \text{ mg m}^{-2}$ . An  
223 eruption at 44 BCE, which is prominent in Greenland records, was recently identified with the Alaskan Okmok eruption  
224 (McConnell et al., 2020), which has been assigned a magnitude of 6.7. The most likely candidate for this eruption in our EDC  
225 record has a deposition of  $15 \text{ mg m}^{-2}$ , identical to the value previously noted for this eruption in Antarctica (Sigl et al., 2015).  
226 It is therefore likely that for eruptions at high northern latitudes our threshold is closer to  $M > 7$ .

227 Using our base set of parameters (200 year median calculation, 30 cm summation of layers per volcano, missing values treated  
228 as having background concentration), we find that the last 200 kyr contains 678 volcanic events with deposition rates greater  
229 than  $20 \text{ mg m}^{-2}$  (Fig. 4); this gives an average of 3.4 per millennium. Although our method is identical in concept, we calculate  
230 rather more peaks greater than  $20 \text{ mg m}^{-2}$  (2.87/ka vs 2.21/kyr) for the period 9-60 ka than that estimated for EDC by previous  
231 work (Lin et al., 2022). This difference seems to arise because our method calculates higher integrals for smaller peaks,  
232 suggesting that the difference is related to the way that the background is calculated and/or the way that we deal with the width  
233 of each peak. This is supported by the fact that at the extreme of our parameter choices (20 cm peak widths, and 100 year  
234 interval for calculating the median background) our estimates converge with those of the previous work (Lin et al., 2022).  
235 There are only 76 peaks with fluxes larger than that of Rinjani/Samalas (1257), making this a 1 in 2500 year event. A time  
236 series of all eruptions greater than  $20 \text{ mg m}^{-2}$  is shown in Fig. 5.

237 Our results are also consistent with independent estimates of the global magnitude-frequency relationship (Rougier et al.,  
238 2018). Based on data shown in Table 4, sulfate peaks  $> 20 \text{ mg m}^{-2}$  should have magnitudes  $\geq 6.5$  while sulfate peaks  $> 50 \text{ mg}$   
239  $\text{m}^{-2}$  should have magnitudes  $\geq 7$ . The analysis of global terrestrial data (Rougier et al., 2018) gives an estimate of  $M \geq 6.5$   
240 eruptions as 2.75/kyr (confidence interval (CI) 1.6-4.3) and an estimate of  $M \geq 7$  eruptions as 0.8/kyr (CI 0.48 to 1.47). Thus  
241 the event rates based on sulfate events at  $> 20 \text{ mg m}^{-2}$  (3.4/kyr) and  $> 50 \text{ mg m}^{-2}$  (0.78/kyr) are well within the uncertainty  
242 ranges of the estimates from the global terrestrial record.

243 The largest peaks in the past 200 kyr deposited around  $300 \text{ mg m}^{-2}$ . The largest recorded eruption in the timeframe that could  
244 accommodate the Toba eruption (Crick et al., 2021; Svensson et al., 2013) has a flux of  $133 \text{ mg m}^{-2}$  (16<sup>th</sup> largest in our record),  
245 This raises questions as to whether, in terms of global dispersion of sulfate aerosol, Toba was the most significant volcanic  
246 climate forcing event of the past 200 kyr. However additional data from other deep ice cores covering this time period are  
247 needed to determine this more certainly.

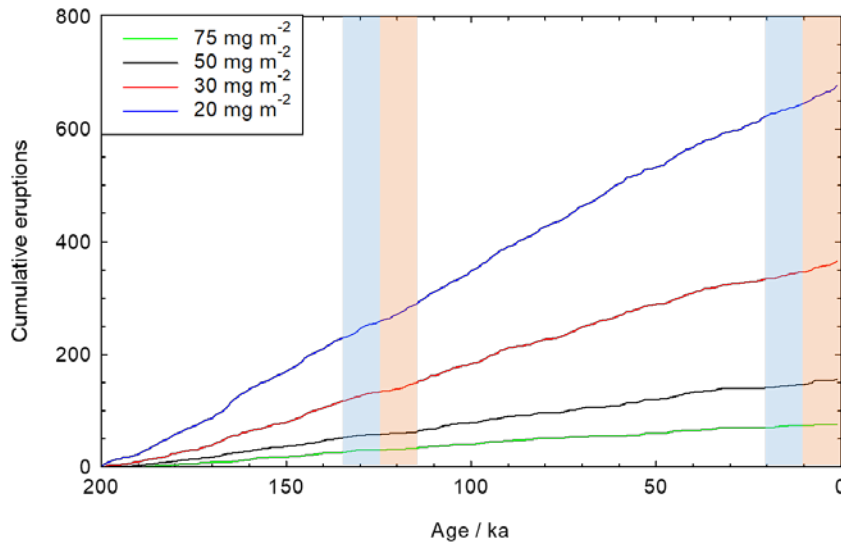


248

249 Figure 5. The deposition flux of sulfate for events with deposition more than  $20 \text{ mg m}^{-2}$  over the last 200 kyr (blue, left axis).  
 250 Antarctic  $\delta\text{D}$  is shown in red (right axis) to indicate the climatic context..

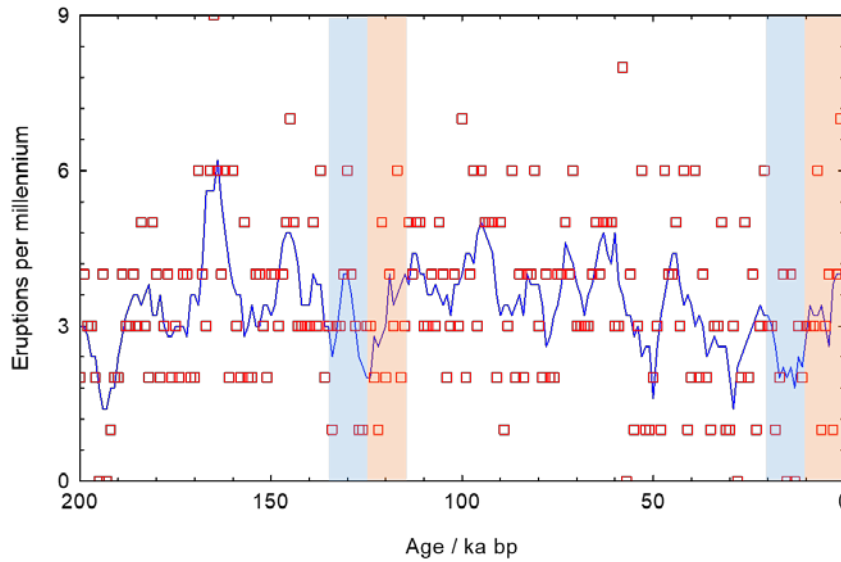
251 To assess whether there are particular periods with high or low numbers of eruptions, we plot the cumulative number of large  
 252 sulfate deposition events with time (Figure 6). Concentrating mainly on the result for eruptions greater than  $20 \text{ mg m}^{-2}$  because  
 253 of the greater numbers involved, the trend is linear, indicating a steady state of large explosive eruptions across two glacial  
 254 cycles. There is no sign of an increased slope (i.e., increased eruption frequency) at the two periods of deglaciation or  
 255 interglacials. This can be seen in Fig. 7. The number of eruptions per millennium is very variable, as is to be expected from  
 256 counting statistics for such small numbers. As a result the time series plot of the occurrence data is very scattered (Fig. 7).  
 257 Nonetheless it is quite obvious that, at Dome C, both periods of deglaciation tend to have eruption frequencies at the lower  
 258 end of the range, rather than increased rates.

259



260

261 Figure 6: Cumulative eruption numbers over the past 200 kyr recorded in the Dome C ice core for different eruption deposition fluxes of  
 262 sulfate. Periods of deglaciation marked with blue bar, interglacials with orange bar.



263

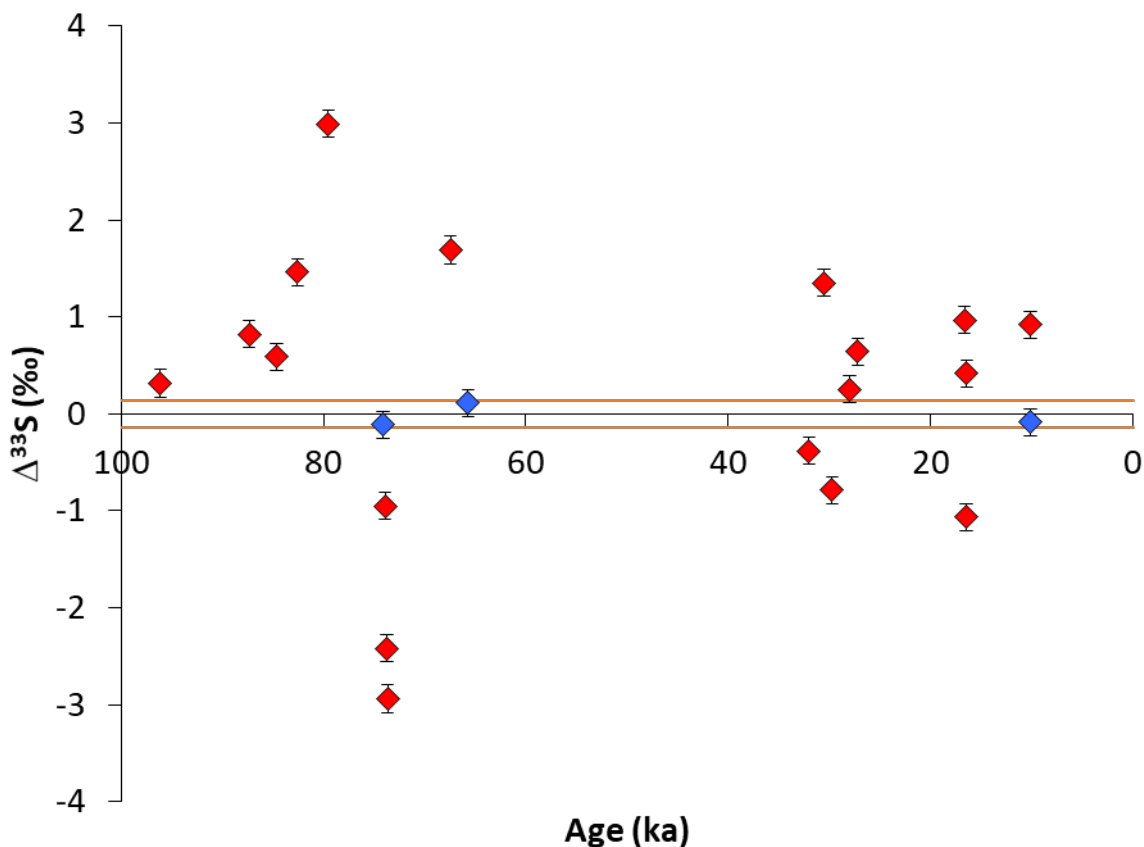
264 Figure 7: Eruption numbers per millennium (red) and 5 kyr running mean (blue). Periods of deglaciation marked with blue  
 265 bar, interglacials with orange bar.

266 We explored other ways of analysing the ice core data to assess whether a climate cycle signal can be recognised. Using  
 267 spectral analysis on the millennial eruption counts, we identified a possible peak corresponding to a 20 kyr period (frequency  
 268 similar to precession) that emerges with weak statistical significance. This certainly needs to be confirmed in other records.

269 Although there have been weak indications of a 23 kyr period in Mediterranean tephra data (Kutterolf et al., 2019) it is difficult  
270 to envisage a mechanism by which precession would influence global volcanism, given that it leads to much weaker changes  
271 in ice sheet unloading and sea level compared to the longer (of order 100 kyr) period. Temperature and snow accumulation  
272 rate at the EDC site show only very weak precessional power (Jouzel et al., 2007), so precessional changes in deposition  
273 efficiency are unlikely to be strong. However, precession significantly influences tropical hydroclimate and the position and  
274 width of the ITCZ (Singarayer et al., 2017). These changes could affect the washout of aerosol from eruptions in tropical  
275 regions, and hence their ability to reach the stratosphere. There will certainly also be an associated effect on the efficiency of  
276 the Brewer Dobson circulation that transports aerosol to the poles through the stratosphere, although we are not aware of model  
277 simulations of this transport involving significant changes in precession (Fu et al., 2020). Thus, if the 20 kyr period is confirmed  
278 it might be ascribed to a small change in the effectiveness of transporting tropical or Northern Hemisphere eruption material  
279 to Antarctica. We emphasise that there is no significant signal at the lower Milankovitch frequency corresponding to 40 kyr.  
280 Our record is too short to make a meaningful assessment in frequency space of the ~100 kyr cycle on which deglaciations  
281 occur, but we again emphasise that, if anything, we see lower numbers of recorded events across the two deglaciations.

## 282 **5. Discussion**

283 As described earlier, there are several challenges when interpreting this dataset as a record of global volcanism. First, there is  
284 the difficulty of separating local tropospheric from larger magnitude stratospheric eruptions. Mass-independent sulfur isotopes  
285 in ice cores can be used to determine whether a volcanic event was stratospheric (Baroni et al., 2008; Burke et al., 2019;  
286 Gautier et al., 2019; Savarino et al., 2003b). Isotope analysis of large sulfate peaks from the last 2600 years at Dome C (Gautier  
287 et al., 2019) indicates 11 tropospheric and 49 stratospheric events, with 4 events showing an inconclusive signal. All the  
288 largest events ( $>20 \text{ mg m}^{-2}$  deposited at Dome C) were stratospheric. In this study, we tested if the proportion of stratospheric  
289 events recorded at Dome C was the same earlier in the record by measuring an additional 21 events from Dome C between  
290 10.1 and 96.1 ka following previous methods (Burke et al., 2019). Mass-independent fractionation of S occurs when sulfur  
291 dioxide is photo-oxidised above the ozone layer, producing positive values of  $\Delta^{33}\text{S}$ , followed by (for reasons of mass balance)  
292 negative values, so that non-zero values of either sign indicate material that has reached the stratosphere. We found (Fig. 8 and  
293 supplementary table) that most (18 out of 21; 15 out of 17 for deposition  $>20 \text{ mg m}^{-2}$ ) volcanic signals in Dome C are  
294 stratospheric, consistent with its isolated location away from most volcanic sources. The sulfur isotope data therefore show  
295 that more than 80% of the volcanic events recorded at Dome C involved stratospheric input due to large explosive eruptions.



296

297 Fig. 8. Values of  $\Delta^{33}\text{S}$  for 21 large volcanic eruptions recorded at Dome C in the last 100 kyr. Values outside a range of  $\pm 0.14\text{‰}$   
 298 are considered to indicate a stratospheric eruption.

299 Second, sulfate peak amplitudes can vary strongly between core sites that are close together, and major peaks can even be  
 300 missing at a single site (Gautier et al., 2016; Wolff et al., 2005). This problem is particularly pronounced at sites with low  
 301 snow accumulation where years may be missing, like Dome C (Wolff et al., 2005), but these sites must be used to investigate  
 302 long records of volcanism. This issue will cause variability in measured eruption rates which should average out over longer  
 303 time periods.

304 Third, there will be a significant bias in the record of global explosive volcanism in Antarctica as a consequence of source  
 305 locations and magnitude. Northern Hemisphere extratropical eruptions ( $>23^\circ\text{N}$ ) will be under-represented and biased towards  
 306 very large eruptions with the likelihood of sulfate aerosol moving into the Southern Hemisphere being a function of source  
 307 latitude and magnitude (Marshall et al., 2021). Thus the Antarctic volcanic record will be biased by larger depositional fluxes  
 308 for tropical and especially Southern Hemisphere extratropical sources while exhibiting smaller depositional fluxes or even  
 309 missing events for Northern Hemisphere extratropical eruptions.

310 The bias in source locations with extratropical Northern Hemisphere eruptions being underrepresented may result in net under-  
311 recording. The estimates of Sigl et al. (Sigl et al., 2015) suggest that around 80% of eruptions giving the greatest global aerosol  
312 loadings are recorded in Antarctica. Our Antarctic ice core data therefore might underestimate the number of eruptions in each  
313 size class by perhaps 20%, somewhat compensated by the ~20% of eruptions from regional volcanoes recorded in Antarctica  
314 that are tropospheric (Gautier et al., 2019). To first order, both the over-recording due to tropospheric eruptions and the under-  
315 recording of extratropical northern hemisphere eruptions should operate in a similar way through time (excluding any effects  
316 of changing transport strength discussed above) and across a range of eruption magnitudes. Thus the shape of the plots of  
317 number of eruptions versus time and of number against sulfur deposition should be unaffected.

318 Finally the ice core record in Antarctica is a record of large silicic explosive eruptions (likely mostly  $M > 6.5$ ). A spatial  
319 analysis of the LaMEVE database of Quaternary explosive eruptions (Fig. 1 in Brown et al., 2014) show that the sources of  
320 these big eruptions are largely in low and mid latitudes. This spatial bias is a consequence of present day plate boundary  
321 distributions. Tectonic settings conducive to forming large silicic magma reservoirs and characterised by caldera forming large  
322 magnitude explosive eruptions are typically in low and mid latitudes where deglaciation effects on melt generation are likely  
323 to be absent or greatly reduced. There are no known  $M > 7$  Quaternary eruption from a northern high latitude volcano ( $>60^\circ\text{N}$ )  
324 (Brown et al., 2014). Thus our findings are not necessarily in contradiction to previous findings (such as Huybers and  
325 Langmuir, 2009) because the Antarctic record is biased towards silicic explosive eruption in the southern hemisphere and  
326 tropical regions.

## 327 **6. Conclusions**

328 In this study we have extended the study of explosive eruptions recorded at the EDC ice core to 200 ka BP, using a method  
329 that should consistently record large volcanic events through time. The record mainly represents large magnitude explosive  
330 eruptions with magnitudes of 6.5 or above. We find no systematic variability through time, though there could be a small effect  
331 of transport efficiency manifested in an apparent 20 kyr period that needs to be confirmed in other cores. There is no sign of  
332 any increase in eruption frequency at deglaciations. This does not of course negate the likelihood that unloading of ice did  
333 cause increased frequencies in regions susceptible to such effects, such as Iceland. However, taking into account the S isotope  
334 evidence that most large eruptions recorded at EDC are stratospheric, our record is probably representative for the major events  
335 influencing climate through stratospheric sulfate. We cannot rule out an effect from volcanism on the balance of  $\text{CO}_2$   
336 production and removal at deglaciation (Huybers and Langmuir, 2009), but it would have to operate only through smaller high  
337 latitude eruptions and/or submarine volcanism. Finally we comment that it is difficult to study volcanism in ice cores over a  
338 period longer than 200 ka until the post-depositional effects leading to artefact peaks are better understood.

## 339 **Data availability**



340 The sulfate data on which this paper is based are available at the NCEI paleoclimate data center, at  
341 <https://www.ncdc.noaa.gov/paleo-search/study/31332>; the depths and ages of large volcanic peaks in the EDC ice core that  
342 form the basis for Figures 5-7 are listed at Wolff, Eric W; Severi, Mirko (2021): Fluxes of largest volcanic peaks in the EDC  
343 sulfate record. PANGAEA, <https://doi.org/10.1594/PANGAEA.926087>

344 The age model data, including accumulation rate and thinning factor, is available in the supplement to the Bazin et al. (2013)  
345 and in the Pangaea database at <https://doi.org/10.1594/PANGAEA.824865>

346 The code used to identify, sum and count peaks, as well as the input data file, is attached as a supplement to this paper.

#### 347 **Author contribution**

348 EW, AB and RSJS conceived the idea for this paper. MS provided the sulfate data that were analysed by the Firenze laboratory.  
349 EW and SHM studied the ice core data to determine which samples should undergo S isotope analysis. SHM, EAD and LC  
350 prepared the samples for S isotope analysis, while AB, HMI and LC carried out those analyses. EWW developed and  
351 implemented the sulfate peak identification method, analysed and sensitivity tested the data. AB and JWBR investigated the  
352 spectral properties of the data. RSJS and SHM advised about the nature of the volcanic record, including marine and terrestrial  
353 data. RSJS, EWW and AB prepared sections of text and all authors edited the text.

#### 354 **Competing interests**

355 One of the authors is a member of the CP editorial board. The authors declare that they have no other conflicts of interest.

#### 356 **Acknowledgments**

357 This project has been supported by the Leverhulme Trust (RPG-2015-246), by a Royal Society Professorship to EWW, and  
358 by a Marie Curie Career Integration Grant to AB. This work is a contribution to the European Project for Ice Coring in  
359 Antarctica (EPICA), a joint European Science Foundation/European Commission (EC) scientific programme, funded by the  
360 EU and by national contributions from Belgium, Denmark, France, Germany, Italy, The Netherlands, Norway, Sweden,  
361 Switzerland and the UK. The main logistic support at Dome C was provided by IPEV and PNRA. We thank Michael Sigl for  
362 help with data on estimated emissions of SO<sub>2</sub>.

#### 363 **Financial support**

364 This research has been supported by the Leverhulme Trust (grant RPG-2015-246), by a Royal Society Professorship (grant no.  
365 RP/R/180003), and by a Marie Curie Career Integration Grant (CIG14-631752).

#### 366 **Figure captions**

367 Figure 1. Comparison of FIC and IC data for two sections of the EDC ice core. In the section from 130 to 150 m, FIC peaks are consistently  
368 lower than those of IC while in the section from 390 metres, the concentrations are the same in the two methods.

369 Figure 2. Examples of volcanic peaks at different depths and ages. The 1257 peak (top panel) is shown after application of the  
370 correction described above. The black horizontal bar on each plot represents 5 years at each depth. Dots represent the mid-  
371 depths of individual samples.

372 Figure 3. An example of four artefact peaks in ice aged just over 400 ka.

373 Figure 4. Distribution of positive and negative peaks exceeding different deposition fluxes, summed over the past 200 kyr.

374 Figure 5. The deposition flux of sulfate for events with deposition more than  $20 \text{ mg m}^{-2}$  over the last 200 kyr.

375 Figure 6: Cumulative eruption numbers over the past 200 kyr recorded in the Dome C ice core for different eruption deposition  
376 fluxes of sulfate. Periods of deglaciation marked with blue bar, interglacials with orange bar.

377 Figure 7: Eruption numbers per millennium (red) and 5 kyr running mean (blue). Periods of deglaciation marked with blue  
378 bar, interglacials with orange bar.

379 Fig. 8. Values of  $\Delta^{33}\text{S}$  for 21 large volcanic eruptions recorded at Dome C in the last 100 kyr. Values outside a range of  $\pm 0.14\%$   
380 are considered to indicate a stratospheric eruption.

381

## 382 **References**

383

384 Barnes, P. R. F., Wolff, E. W., Mader, H. M., Udisti, R., Castellano, E., and Rothlisberger, R.: Evolution of chemical peak shapes in the  
385 Dome C, Antarctica, ice core, *J. Geophys. Res.*, 108, doi:10.1029/2002JD002538, 2003.

386

387 Baroni, M., Savarino, J., Cole-Dai, J. H., Rai, V. K., and Thiemens, M. H.: Anomalous sulfur isotope compositions of volcanic sulfate over  
388 the last millennium in Antarctic ice cores, *J. Geophys. Res.-Atmos.*, 113, doi: 10.1029/2008jd010185, 2008.

389

390 Bazin, L., Landais, A., Lemieux-Dudon, B., Kele, H. T. M., Veres, D., Parrenin, F., Martinerie, P., Ritz, C., Capron, E., Lipenkov, V.,  
391 Loutre, M. F., Raynaud, D., Vinther, B., Svensson, A., Rasmussen, S. O., Severi, M., Blunier, T., Leuenberger, M., Fischer, H., Masson-  
392 Delmotte, V., Chappellaz, J., and Wolff, E. W.: An optimised multi-proxy, multi-site Antarctic ice and gas orbital chronology (AICC2012):  
393 120-800 ka, *Climate of the Past* 9, 1715-1731, 2013.

394

395 Brown, S. K., Croswell, H. S., Sparks, R. S. J., Cottrell, E., Deligne, N. I., Guerrero, N. O., Hobbs, L., Kiyosugi, K., Loughlin, S. C.,  
396 Siebert, L., and Takarada, S.: Characterisation of the Quaternary eruption record: analysis of the Large Magnitude Explosive Volcanic  
397 Eruptions (LaMEVE) database, *Journal of Applied Volcanology*, 3, 5, doi: 10.1186/2191-5040-3-5, 2014.

398

399 Burke, A., Moore, K. A., Sigl, M., Nita, D. C., McConnell, J. R., and Adkins, J. F.: Stratospheric eruptions from tropical and extra-tropical  
400 volcanoes constrained using high-resolution sulfur isotopes in ice cores, *Earth planet. Sci. Lett.*, 521, 113-119, doi:  
401 <https://doi.org/10.1016/j.epsl.2019.06.006>, 2019.

402

403 Castellano, E., Becagli, S., Hansson, M., Hutterli, M., Petit, J. R., Rampino, M. R., Severi, M., Steffensen, J. P., Traversi, R., and Udisti, R.:  
404 Holocene volcanic history as recorded in the sulfate stratigraphy of the European Project for Ice Coring in Antarctica Dome C (EDC96) ice  
405 core, *J. Geophys. Res.*, 110, D06114, doi:06110.01029/02004JD005259, 2005.

406

407 Castellano, E., Becagli, S., Jouzel, J., Migliori, A., Severi, M., Steffensen, J. P., Traversi, R., and Udisti, R.: Volcanic eruption frequency  
408 over the last 45 ky as recorded in Epica-Dome C ice core (East Antarctica) and its relationship with climatic changes, *Global and Planetary*  
409 *Change*, 42, 195-205, 2004.

410

411 Cole-Dai, J., Ferris, D. G., Kennedy, J. A., Sigl, M., McConnell, J. R., Fudge, T. J., Geng, L., Maselli, O. J., Taylor, K. C., and Souney, J.  
412 M.: Comprehensive Record of Volcanic Eruptions in the Holocene (11,000 years) From the WAIS Divide, Antarctica Ice Core, *Journal of*  
413 *Geophysical Research: Atmospheres*, 126, e2020JD032855, doi: <https://doi.org/10.1029/2020JD032855>, 2021.

414

415 Cole-Dai, J. and Mosley-Thompson, E.: The Pinatubo eruption in South Pole snow and its potential value to ice-core paleovolcanis records,  
416 *Ann. Glaciol.*, 29, 99-105, 1999.

417

418 Crick, L., Burke, A., Hutchison, W., Kohno, M., Moore, K. A., Savarino, J., Doyle, E. A., Mahony, S., Kipfstuhl, S., Rae, J. W. B., Steele,  
419 R. C. J., Sparks, R. S. J., and Wolff, E. W.: New insights into the ~ 74ka Toba eruption from sulfur isotopes of polar ice cores, *Clim. Past*,  
420 17, 2119-2137, doi: 10.5194/cp-17-2119-2021, 2021.

421

422 Fu, Q., White, R. H., Wang, M., Alexander, B., Solomon, S., Gettelman, A., Battisti, D. S., and Lin, P.: The Brewer-Dobson Circulation  
423 During the Last Glacial Maximum, *Geophys. Res. Lett.*, 47, e2019GL086271, doi: <https://doi.org/10.1029/2019GL086271>, 2020.

424

425 Fujita, S., Parrenin, F., Severi, M., Motoyama, H., and Wolff, E. W.: Volcanic synchronization of Dome Fuji and Dome C Antarctic deep  
426 ice cores over the past 216 kyr, *Clim. Past*, 11, 1395-1416, doi: 10.5194/cp-11-1395-2015, 2015.

427

428 Gao, C., Robock, A., and Ammann, C.: Volcanic forcing of climate over the past 1500 years: An improved ice core-based index for climate  
429 models, *J. Geophys. Res.*, 113, D23111, 2008.

430

431 Gautier, E., Savarino, J., Erbland, J., Lanciki, A., and Possenti, P.: Variability of sulfate signal in ice core records based on five replicate  
432 cores, *Climate of the Past*, 12, 103-113, doi: 10.5194/cp-12-103-2016, 2016.

433

434 Gautier, E., Savarino, J., Hoek, J., Erbland, J., Caillon, N., Hattori, S., Yoshida, N., Albalat, E., Albarede, F., and Farquhar, J.: 2600-years  
435 of stratospheric volcanism through sulfate isotopes, *Nature Communications*, 10, 466, doi: 10.1038/s41467-019-08357-0, 2019.

436

437 Huybers, P. and Langmuir, C.: Feedback between deglaciation, volcanism, and atmospheric CO<sub>2</sub>, *Earth planet. Sci. Lett.*, 286, 479-491, doi:  
438 10.1016/j.epsl.2009.07.014, 2009.

439

440 Jouzel, J., Masson-Delmotte, V., Cattani, O., Dreyfus, G., Falourd, S., Hoffmann, G., Nouet, J., Barnola, J. M., Chappellaz, J., Fischer, H.,  
441 Gallet, J. C., Johnsen, S., Leuenberger, M., Loulergue, L., Luethi, D., Oerter, H., Parrenin, F., Raisbeck, G., Raynaud, D., Schwander, J.,  
442 Spahni, R., Souchez, R., Selmo, E., Schilt, A., Steffensen, J. P., Stenni, B., Stauffer, B., Stocker, T., Tison, J.-L., Werner, M., and Wolff, E.  
443 W.: Orbital and millennial Antarctic climate variability over the last 800 000 years, *Science*, 317, 793-796, doi: 10.1126/science.1141038,  
444 2007.

445

446 Jull, M. and McKenzie, D.: The effect of deglaciation on mantle melting beneath Iceland, *J. Geophys. Res.-Solid Earth*, 101, 21815-21828,  
447 doi: 10.1029/96jb01308, 1996.

448

449 Kutterolf, S., Schindlbeck, J. C., Jegen, M., Freundt, A., and Straub, S. M.: Milankovitch frequencies in tephra records at volcanic arcs: The  
450 relation of kyr-scale cyclic variations in volcanism to global climate changes, *Quat. Sci. Rev.*, 204, 1-16, doi:  
451 10.1016/j.quascirev.2018.11.004, 2019.

452

453 Legrand, M. and Delmas, R. J.: The ionic balance of Antarctic snow: a 10-year detailed record, *Atmos. Environ.*, 18, 1867-1874, doi:  
454 10.1016/0004-6981(84)90363-9, 1984.

455

456 Lin, J., Svensson, A., Hvidberg, C. S., Lohmann, J., Kristiansen, S., Dahl-Jensen, D., Steffensen, J. P., Rasmussen, S. O., Cook, E., Kjør,  
457 H. A., Vinther, B. M., Fischer, H., Stocker, T., Sigl, M., Bigler, M., Severi, M., Traversi, R., and Mulvaney, R.: Magnitude, frequency and  
458 climate forcing of global volcanism during the last glacial period as seen in Greenland and Antarctic ice cores (60–9 ka), *Clim. Past*, 18,  
459 485-506, doi: 10.5194/cp-18-485-2022, 2022.

460

461 Littot, G. C., Mulvaney, R., Rothlisberger, R., Udisti, R., Wolff, E. W., Castellano, E., de Angelis, M., Hansson, M., Sommer, S., and  
462 Steffensen, J. P.: Comparison of analytical methods used for measuring major ions in the EPICA Dome C (Antarctica) ice core, *Ann. Glaciol.*,  
463 35, 299-305, 2002.

464

465 Mahony, S. H., Barnard, N. H., Sparks, R. S. J., and Rougier, J. C.: VOLCORE, a global database of visible tephra layers sampled by ocean  
466 drilling, *Scientific Data*, 7, doi: 10.1038/s41597-020-00673-1, 2020.

467  
468 Marshall, L. R., Schmidt, A., Johnson, J. S., Mann, G. W., Lee, L. A., Rigby, R., and Carslaw, K. S.: Unknown Eruption Source Parameters  
469 Cause Large Uncertainty in Historical Volcanic Radiative Forcing Reconstructions, *Journal of Geophysical Research: Atmospheres*, 126,  
470 e2020JD033578, doi: <https://doi.org/10.1029/2020JD033578>, 2021.

471  
472 McConnell, J. R., Burke, A., Dunbar, N. W., Köhler, P., Thomas, J. L., Arienzo, M. M., Chellman, N. J., Maselli, O. J., Sigl, M., Adkins, J.  
473 F., Bagginstos, D., Burkhardt, J. F., Brook, E. J., Buizert, C., Cole-Dai, J., Fudge, T. J., Knorr, G., Graf, H.-F., Grieman, M. M., Iverson, N.,  
474 McGwire, K. C., Mulvaney, R., Paris, G., Rhodes, R. H., Saltzman, E. S., Severinghaus, J. P., Steffensen, J. P., Taylor, K. C., and Winckler,  
475 G.: Synchronous volcanic eruptions and abrupt climate change ~17.7 ka plausibly linked by stratospheric ozone depletion, *Proceedings of*  
476 *the National Academy of Sciences*, 114, 10035-10040, doi: 10.1073/pnas.1705595114, 2017.

477  
478 McConnell, J. R., Sigl, M., Plunkett, G., Burke, A., Kim, W. M., Raible, C. C., Wilson, A. I., Manning, J. G., Ludlow, F., Chellman, N. J.,  
479 Innes, H. M., Yang, Z., Larsen, J. F., Schaefer, J. R., Kipfstuhl, S., Mojtavavi, S., Wilhelms, F., Opel, T., Meyer, H., and Steffensen, J. P.:  
480 Extreme climate after massive eruption of Alaska's Okmok volcano in 43 BCE and effects on the late Roman Republic and Ptolemaic  
481 Kingdom, *Proc. Natl. Acad. Sci. U. S. A.*, 117, 15443-15449, doi: 10.1073/pnas.2002722117, 2020.

482  
483 Parrenin, F., Petit, J.-R., Masson-Delmotte, V., Basile, I., Jouzel, J., Lipenkov, V., Rasmussen, S., Schwander, J., Severi, M., Udisti, R.,  
484 Veres, D., Vinther, B., and Wolff, E. W.: Volcanic synchronisation between the EPICA Dome C and Vostok ice cores  
485 (Antarctica) 0-145 kyr BP, *Climate of the Past* 8, 1031-1045, 2012.

486  
487 Patris, N., Delmas, R. J., and Jouzel, J.: Isotopic signatures of sulfur in shallow Antarctic ice cores, *J. Geophys. Res.-Atmos.*, 105, 7071-  
488 7078, 2000.

489  
490 Robock, A.: Volcanic eruptions and climate, *Rev. Geophys.*, 38, 191-219, doi: doi:10.1029/1998RG000054, 2000.

491  
492 Rougier, J., Sparks, R. S. J., Cashman, K. V., and Brown, S. K.: The global magnitude–frequency relationship for large explosive volcanic  
493 eruptions, *Earth planet. Sci. Lett.*, 482, 621-629, doi: <https://doi.org/10.1016/j.epsl.2017.11.015>, 2018.

494  
495 Ruth, U., Barnola, J. M., Beer, J., Bigler, M., Blunier, T., Castellano, E., Fischer, H., Fundel, F., Huybrechts, P., Kaufmann, P., Kipfstuhl,  
496 J., Lambrecht, A., Morganti, A., Oerter, H., Parrenin, F., Rybak, O., Severi, M., Udisti, R., Wilhelms, F., and Wolff, E. W.: "EDML1": A  
497 chronology for the EPICA deep ice core from Dronning Maud Land, Antarctica, over the last 150,000 years, *Climate of the Past*, 3, 475-  
498 484, 2007.

499  
500 Savarino, J., Bekki, S., Cole-Dai, J. H., and Thiemens, M. H.: Evidence from sulfate mass independent oxygen isotopic compositions of  
501 dramatic changes in atmospheric oxidation following massive volcanic eruptions, *J. Geophys. Res.*, 108, 4671, 2003a.

502  
503 Savarino, J., Romero, A., Cole-Dai, J., Bekki, S., and Thiemens, M. H.: UV induced mass-independent sulfur isotope fractionation in  
504 stratospheric volcanic sulfate, *Geophys. Res. Lett.*, 30, doi: 10.1029/2003gl018134, 2003b.

505  
506 Severi, M., Becagli, S., Traversi, R., and Udisti, R.: Recovering Paleo-Records from Antarctic Ice-Cores by Coupling a Continuous Melting  
507 Device and Fast Ion Chromatography, *Analyt. Chem.*, 87, 11441-11447, doi: 10.1021/acs.analchem.5b02961, 2015.

508  
509 Sigl, M., McConnell, J. R., Layman, L., Maselli, O., McGwire, K., Pasteris, D., Dahl-Jensen, D., Steffensen, J. P., Vinther, B., Edwards, R.,  
510 Mulvaney, R., and Kipfstuhl, S.: A new bipolar ice core record of volcanism from WAIS Divide and NEEM and implications for climate  
511 forcing of the last 2000 years, *Journal of Geophysical Research: Atmospheres*, 118, 1151-1169, doi: <https://doi.org/10.1029/2012JD018603>,  
512 2013.

513  
514 Sigl, M., Toohey, M., McConnell, J. R., Cole-Dai, J., and Severi, M.: Volcanic stratospheric sulfur injections and aerosol optical depth  
515 during the Holocene (past 11500 years) from a bipolar ice-core array, *Earth Syst. Sci. Data*, 14, 3167-3196, doi: 10.5194/essd-14-3167-2022,  
516 2022.

517  
518 Sigl, M., Winstrup, M., McConnell, J. R., Welten, K. C., Plunkett, G., Ludlow, F., Buntgen, U., Caffee, M., Chellman, N., Dahl-Jensen, D.,  
519 Fischer, H., Kipfstuhl, S., Kostick, C., Maselli, O. J., Mekhaldi, F., Mulvaney, R., Muscheler, R., Pasteris, D. R., Pilcher, J. R., Salzer, M.,  
520 Schupbach, S., Steffensen, J. P., Vinther, B. M., and Woodruff, T. E.: Timing and climate forcing of volcanic eruptions for the past 2,500  
521 years, *Nature*, 523, 543-+, doi: 10.1038/nature14565, 2015.

522

523 Singarayer, J. S., Valdes, P. J., and Roberts, W. H. G.: Ocean dominated expansion and contraction of the late Quaternary tropical rainbelt,  
524 Scientific Reports, 7, 9382, doi: 10.1038/s41598-017-09816-8, 2017.  
525

526 Svensson, A., Bigler, M., Blunier, T., Clausen, H. B., Dahl-Jensen, D., Fischer, H., Fujita, S., Goto-Azuma, K., Johnsen, S. J., Kawamura,  
527 K., Kipfstuhl, S., Kohno, M., Parrenin, F., Popp, T., Rasmussen, S. O., Schwander, J., Seierstad, I., Severi, M., Steffensen, J. P., Udisti, R.,  
528 Uemura, R., Vallelonga, P., Vinther, B. M., Wegner, A., Wilhelms, F., and Winstrup, M.: Direct linking of Greenland and Antarctic ice  
529 cores at the Toba eruption (74 ka BP), *Clim. Past*, 9, 749-766, doi: 10.5194/cp-9-749-2013, 2013.  
530

531 Toohey, M. and Sigl, M.: Volcanic stratospheric sulfur injections and aerosol optical depth from 500 BCE to 1900 CE, *Earth Syst. Sci. Data*,  
532 9, 809-831, doi: 10.5194/essd-9-809-2017, 2017.  
533

534 Traversi, R., Becagli, S., Castellano, E., Marino, F., Rugi, F., Severi, M., Angelis, M. d., Fischer, H., Hansson, M., Stauffer, B., Steffensen,  
535 J. P., Bigler, M., and Udisti, R.: Sulfate Spikes in the Deep Layers of EPICA-Dome C Ice Core: Evidence of Glaciological Artifacts,  
536 *Environmental Science & Technology*, 43, 8737-8743, doi: 10.1021/es901426y, 2009.  
537

538 Wallace, P. J. and Edmonds, M.: The Sulfur Budget in Magmas: Evidence from Melt Inclusions, Submarine Glasses, and Volcanic Gas  
539 Emissions, *Reviews in Mineralogy and Geochemistry*, 73, 215-246, doi: 10.2138/rmg.2011.73.8, 2011.  
540

541 Watt, S. F. L., Pyle, D. M., and Mather, T. A.: The volcanic response to deglaciation: Evidence from glaciated arcs and a reassessment of  
542 global eruption records, *Earth-Sci. Rev.*, 122, 77-102, doi: 10.1016/j.earscirev.2013.03.007, 2013.  
543

544 Wolff, E. W.: Electrical stratigraphy of polar ice cores: principles, methods, and findings. In: *Physics of Ice Core Records*, Hondoh, T. (Ed.),  
545 Hokkaido University Press, Sapporo, 2000.  
546

547 Wolff, E. W., Cook, E., Barnes, P. R. F., and Mulvaney, R.: Signal variability in replicate ice cores, *J. Glaciol.*, 51, 462-468, 2005.  
548  
549